Fast and Effective Optimisation of Arrays of Submerged Wave Energy Converters

Junhua Wu*, Slava Shekh*, Nataliia Y. Sergiienko†, Benjamin S. Cazzolato†,
Boyin Ding†, Frank Neumann*, Markus Wagner*
* Optimisation and Logistics Group, †School of Mechanical Engineering
The University of Adelaide, Australia

ABSTRACT

Renewable forms of energy are becoming increasingly important to consider, as the global energy demand continues to grow. Wave energy is one of these widely available forms, but it is largely unexploited. A common design for a wave energy converter is called a point absorber or buoy. The buoy typically floats on the surface or just below the surface of the water, and captures energy from the movement of the waves. It can use the motion of the waves to drive a pump to generate electricity and to create potable water. Since a single buoy can only capture a limited amount of energy, large-scale wave energy production necessitates the deployment of buoys in large numbers called arrays. However, the efficiency of arrays of buoys is affected by highly complex intra-buoy interactions.

The contributions of this article are two-fold. First, we present an approximation of the buoy interactions model that results in a 350-fold computational speed-up to enable the use inside of iterative optimisation algorithms, Second, we study arrays of fully submerged three-tether buoys, with and without shared mooring points.

CCS Concepts

•**Computing methodologies → Heuristic function construction; Randomized search;**

Keywords

Renewable energy; evolutionary algorithm; wave energy

1. INTRODUCTION

Global energy demand is on the rise, and finite reserves of fossil fuels, renewable forms of energy are playing a more and more important role in our energy supply [20]. Wave energy is a widely available but largely unexploited source of renewable energy with the potential to make a substantial contribution to future energy production [8, 16]. The idea of harnessing wave energy has been around for at least two
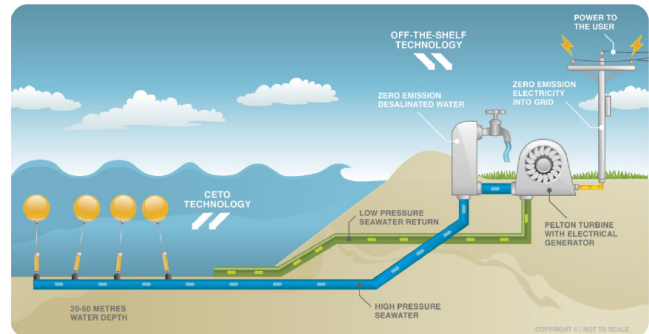
Figure 1: Operation of the CETO system [22].

centuries, with the first patent for a wave energy device being filed in 1799 [9]. However, it was not until the oil crisis of the 1970s and the publication of Stephen Salter's iconic paper in Nature [26] that interest in wave energy truly began to surge. Since that time, the utilisation of wave energy has continued to be a very active research area. There are currently dozens of ongoing wave energy projects at various stages of development, exploring a variety of techniques [8, 9, 16, 19].

A device that captures and converts wave energy to electricity is often referred to as a wave energy device or wave energy converter (WEC). One common WEC design is called a point absorber or buoy. The buoy typically floats on the surface or just below the surface of the water, and captures energy from the movement of the waves [16]. An example of a point absorber is the CETO wave energy converter, developed by Carnegie Wave Energy and named after the Greek sea goddess Ceto [21]. The CETO system consists of one or more fully submerged buoys that are tethered to the seabed in an offshore location, as shown in Figure 1. These buoys use the motion of the waves to drive a hermetically sealed hydraulic line to drive hydroelectric turbines to generate electricity, or to power a reverse osmosis desalination plant to create potable water [22].

One of the central goals in designing and operating a wave energy device is to maximise its overall energy absorption. As a result, the optimisation of various aspects of wave energy converters is an important and active area of research. Three key aspects that are often optimised are geometry, control, and positioning. Geometric optimisation seeks to improve the shape and/or dimensions of a wave energy converter (or some part of it) with the objective of maximising

energy capture [23, 24]. On the other hand, the optimisation of control is concerned with finding good strategies for actively controlling a WEC [25]. A suitable control strategy is needed for achieving high WEC performance in real seas and oceans, due to the presence of irregular waves [13]. In this article we focus on the third aspect, namely the positioning of wave energy converters.

A single wave energy converter can only capture a limited amount of energy alone. For large-scale wave energy production and in order to make any significant contribution to addressing global energy demand, it is essential to deploy wave energy devices in large numbers. A group of wave energy devices working in close proximity to one another is referred to as a wave energy farm or array [7]. Just as the optimisation of individual wave energy devices is an area of research, so is the optimisation of arrays of such devices. In the case of arrays, the aspects that are typically optimised include the layout or configuration of the array [6] and active control of individual devices [12].

In the current body of research on wave energy converter arrays and their optimisation, many of the devices under consideration are semi-submerged or floating [4, 6, 11]. In contrast, the CETO WEC is fully submerged beneath the ocean surface [22], as this increases the survivability in high sea states and it has almost no visual impact. There is very limited research into fully submerged wave energy converters. In particular, we are not aware of any research into optimising the placement or configuration of arrays of fully submerged wave energy converters. With this article, we are addressing this issue.

A technological alternative to single-tether CETO WECs are three-tether WECs as shown in Figure 2. The capital cost of such devices are higher than of conventional single-tether heaving buoys due to the increased number of separate power take-off systems for each tether. The total cost of the three-tether WEC array can be reduced significantly, if the layout allows adjacent devices to share the same mooring points (see Figure 3). In this article, we will investigate array layouts for shared mooring points and layouts without shared mooring points.

In order to evaluate arrays, we use a recently developed frequency domain model for arrays of fully submerged three-tether WECs. This model allows us to investigate different parameters, such as number of devices, array layout and buoy size. The ideal choice of parameters leads to an optimisation problem: what is the best combination of buoy radii and their locations for different array sizes?

The structure of the paper is as follows. We introduce the model of interacting three-tether buoys in Section 2 that we base our investigations on. In Section 3, we describe our speed-ups of the original model, as it is computationally prohibitively expensive for the use in iterative optimisation approaches. Then, we present our experimental results in Section 4, and finish with some concluding remarks.

2. MODEL OF THE THREE-TETHER WEC ARRAY

2.1 System description

The WEC design that we consider is a fully submerged spherical body connected to three tethers that are equally distributed around the buoy hull (Figure 2). Each tether is
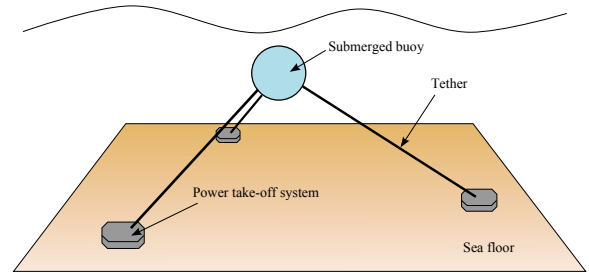

Figure 2: Schematic representation of a three-tether WEC (adapted from [5]).
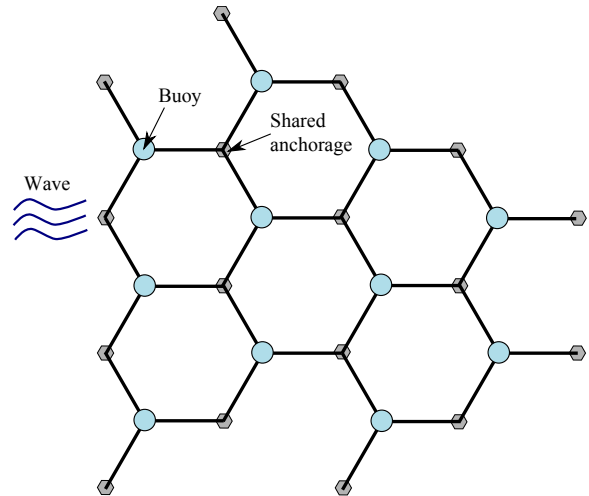

Figure 3: Top view on the array of WECs with shared mooring points.

connected to the individual power generator at the sea floor, which allows to extract power from surge and heave motions simultaneously [27].

The arrangement of a three-tether WEC array may be considered in two different ways:

(i) In arrays where all adjacent devices share common anchorage points and/or power take-off system (see Figure 3). The main benefit of this layout is a significant reduction in the capital cost of the array due to the smaller number of mooring points as compared to the separately placed WECs. At the same time, the optimal buoy placement in such arrays is fixed and depends only on the ocean depth at the particular sea site and desired submergence depth of the buoy [28];

(ii) In arrays where all devices are placed separately (see Figure 2). This layout does not have any constraints on the farm geometry and a buoy placement can be chosen considering various optimisation procedures.

2.2 System dynamics

In the following, we briefly outline the model of this kind of WECs arrays as it was derived by Sergiienko et al. [28].

The dynamic equation of the WECs array is derived in the frequency domain using linear wave theory, where a fluid is inviscid, irrotational and incompressible [10]. This model considers three dominant forces that act on the WECs:

(i) excitation force includes incident and diffracted wave forces when all bodies are assumed to be fixed;

(ii) radiation force acts on the oscillating body due to its own motion in the absence of incident waves;

(iii) control, or power take-off force, that exerts on the WEC from machinery through tethers.

The key point in the array performance is the hydrodynamic interaction between buoys that can be constructive or destructive depending on the array size and geometry.

A spherical body is excited by ocean waves in surge, sway and heave only [18, 29]. However, a geometrical arrangement of a WEC with three tethers induces small angular motions of the body that do not contribute to the power absorption. Therefore, only translational motion of each body is included in the dynamic equation of the system.

Assuming that the total number of devices in the array is N and p is the body number, then the dynamics of the p-th WEC in time domain is described as:

$$\mathbf{M}_p \ddot{\mathbf{x}}_p(t) = \mathbf{F}_{exc,p}(t) + \mathbf{F}_{rad,p}(t) + \mathbf{F}_{pto,p}(t), \quad (1)$$

where $\mathbf{M}_p$ is a mass matrix of the p-th buoy, $\ddot{\mathbf{x}}_p(t)$ is a body acceleration vector in surge, sway and heave, $\mathbf{F}_{exc,p}(t)$, $\mathbf{F}_{rad,p}(t)$, $\mathbf{F}_{pto,p}(t)$ are excitation, radiation and PTO forces respectively. The power take-off system is modelled as a linear spring and damper for each mooring line with two control parameters, such as stiffness K_{pto} and damping coefficient B_{pto}.

In case of multiple bodies, where $p = 1 \ldots N$, Equation (1) can be extended to include all WECs and expressed in frequency domain:

$$\left((\mathbf{M}_\Sigma + \mathbf{A}_\Sigma(\omega)) j\omega + \mathbf{B}_\Sigma(\omega) - \frac{\mathbf{K}_{pto,\Sigma}}{\omega} j + \mathbf{B}_{pto,\Sigma} \right) \hat{\mathbf{x}}_\Sigma$$
$$= \hat{\mathbf{F}}_{exc,\Sigma}, \quad (2)$$

where subscript Σ indicates a generalised vector/matrix for the array of N bodies, $\mathbf{A}_\Sigma(\omega)$ and $\mathbf{B}_\Sigma(\omega)$ are radiation added mass and damping coefficient matrices that include hydrodynamic interaction between buoys, $\mathbf{K}_{pto,\Sigma}$, $\mathbf{B}_{pto,\Sigma}$ are the stiffness and damping block-matrices of the PTO system.

2.3 Performance index

The total power absorbed by the array of WECs can be calculated as:

$$P_\Sigma = \frac{1}{4}(\hat{\mathbf{F}}^*_{exc,\Sigma}\hat{\mathbf{x}}_\Sigma + \hat{\mathbf{x}}^*_\Sigma\hat{\mathbf{F}}_{exc,\Sigma}) - \frac{1}{2}\hat{\mathbf{x}}^*_\Sigma\mathbf{B}\hat{\mathbf{x}}_\Sigma, \quad (3)$$

where * denotes the conjugate transpose.

The performance of an array of N WECs is usually summarised using the so-called q-factor:

$$q = \frac{P_\Sigma}{N \cdot P_0}, \quad (4)$$

where P_0 is the power absorption of a single device in isolation. The q-factor is the ratio of the power absorption of an array of WECs compared to the power absorption of those same converters in isolation. A q-factor greater than one indicates the presence of constructive interference in the array, as the array of devices is producing more energy than the devices would individually. Conversely, a q-factor less than one is a sign of destructive interference, which may be detrimental to the performance of the array.

Lastly, for the fair analysis of layouts that involve WECs of different sizes, we choose the *relative capture width* (RCW) to be a non-dimensional index of power absorption:

$$RCW = \frac{P_\Sigma}{P_w \left(2 \sum_{p=1}^{N} a_p \right)}, \quad (5)$$

where P_w is the incident wave-energy transport per unit frontage, a_p is a radius of the p-th body. RCW shows the fraction of power extracted from the wave per unit length of the device. RCW from Equation (5) is frequency dependent, therefore, for the particular sea site location, the RCW should be weighted according to the sea state probability data. Thus,

$$\overline{RCW} = \frac{\sum_i n_i \cdot RCW(\omega_i)}{\sum_i n_i}, \quad (6)$$

where n_i is an occurrence probability of waves at particular frequency.

2.4 Model specification

In Table 1 we provide the dimensions of the WECs used in the remainder of this article. We choose constant power take-off coefficients to give optimal power for the regular wave of 1m amplitude and 9-second period. The mass of each buoy is equal to 0.85 times the mass of the displaced water. Ocean depth is chosen to be 50m and all WECs are submerged 6m to centre of buoy.

Table 1: Specification of WECs used in array optimisation.

Buoy radius a, m	5	4	3.2	2.5	2
PTO spring coefficient K_{pto}, kN/m	387	185	92	43	22
PTO damping coefficient B_{pto}, kN/(m/sec)	161	76	38	18	8.9

We calculate the hydrodynamic parameters of the WEC array (excitation force, added mass and damping coefficients) based on the algorithm presented by Wu [30]. The results of various array layouts and buoy sizes have been validated against WAMIT [17], which is a computer program for computing wave loads and motions of offshore structures in waves.

3. ARRAY OPTIMISATION

In this section we present our approaches used to speed-up the simulations of the WEC arrays. The techniques include approximations and caching. For an array of 50 WECs, the eventual speed-up is 350-fold, i.e., from approximately 2100 minutes down to six minutes.

3.1 Model Approximation

The model approximation $\mathcal{M}'$ is a substitute of the three-tether model $\mathcal{M}$ with significantly reduced computational cost and acceptable error of accuracy. In terms of accuracy, we create a function p to compare the two models only based on the agreement of their trends. In other words, if the benefit is increasing/decreasing in $\mathcal{M}$ when changing from layout l_1 to layout l_2, we compare whether the same trend
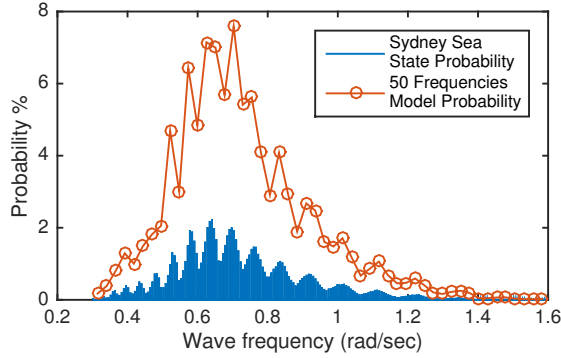
Figure 4: Sydney sea state: historic distribution and 50 samples

Figure 5: Probabilities of frequencies in six approximation models and the original three-tether model

Figure 6: Accuracy of six approximation models for arbitrary layouts. Shown are the results when 10, 5, 4, 3, 2, and only 1 (of 50) frequencies are used.

takes place in the approximation $\mathcal{M}'$. Function p is defined as:

$$p(f(x), x_1, x_2) = \begin{cases} \frac{f(x_1)-f(x_2)}{|f(x_1)-f(x_2)|} & f(x_1) \neq f(x_2) \\ 0 & f(x_1) = f(x_2) \end{cases}$$

Based on the function, a standard binary test is introduced according to the rule that $p(\mathcal{M}', l_1, l_2) = p(\mathcal{M}, l_1, l_2)$ means *positive* and the contrary means *negative*. This way we can compute the accuracy with regard to True Positive, True Negative, False Positive and False Negative.

In order to reduce the computational cost, we consider to reduce the sampling of frequencies. The original variant of the three-tether model utilises 50 sample frequencies to simulate the probability of wave frequencies in reality. In Figure 4, the blue histogram shows the records of different wave frequencies with their probabilities taking place in a sea area close to Sydney [15], and in red we illustrate the 50 evenly chosen frequencies. Each point represents a certain small range of wave frequency and its probability is the sum of the probability of this range. Therefore the total probability of 50 frequencies still sums up to 1, so that the approximate power absorbed by WECs can be calculated by using this simplified version. However, the computation of total power is still costly. The calculation of an array with 50 WECs takes around 35 hours on one core of an Intel Core i5-4250U processor. Since the computation time in linear in the number of considered frequencies, a natural way to the reduce computational cost is to approximate the accurate model with fewer sample frequencies. Our goal is to reduce computation time while keeping the accuracy above 80%.

To achieve this, we create the model approximations with the numbers of sample frequencies to be 10, 5, 4, 3, 2 and 1. Each sample frequency represents a range of actually occurring wave frequencies, and for each approximation we distribute them equally over the spectrum. For the single frequency, however, we select the most likely occurring frequency: 0.7 rad/s. Figure 5 illustrates all the probabilities of frequencies used in the six approximation models compared with the probabilities in the original three-tether model.

We investigate the six approximations in two specific scenarios: 1) arbitrary layouts and 2) evolving layouts. Both of the scenarios are typical in optimisation, especially for evolutionary algorithms. We study layouts with 50 WECs in a one square kilometre rectangular area with a safety constraint that the minimal distance between each pair of WECs must be 50 meters.
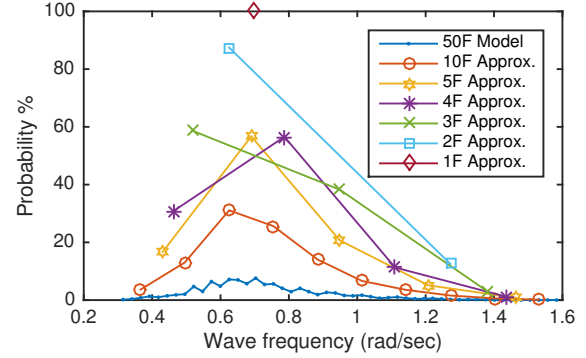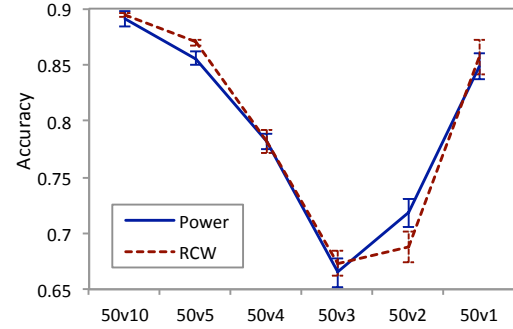
Arbitrary Layouts

In this scenario, we randomly generate 100 valid layouts and divide them into five groups. For each group, we calculate the accuracy between the three-tether model and each of six approximations. Then we plot the averages and standard deviations of the groups of data in Figure 6. As we can see, the two- and three-frequency approximations are the least accurate ones. The fastest model that considers only the prevailing frequency is comparable in accuracy with the one that uses fives frequencies, however, the latter takes fives times as long to compute.

Evolving Layouts

In this scenario we use a simple evolutionary algorithm called (1+1)-EA to study the optimisation using the approximating three-tether model. This algorithm is a hill-climber where new solutions are created based on the best-so-far encountered. If the new solution provides a higher score, then it replaces the best-so-far, otherwise the new solution is discarded; this is repeated until the total time budget is used up. We run 400 generations of the algorithm with a simple mutation which randomly chooses and moves only one WEC in a layout. This optimisation results in an increase of the power output by around 5% (as shown in Figure 7), and it also generates 401 layouts including an initial random layout. We then calculate the accuracy between the original three-tether model and each of six approximations based on the layouts by using the same approach as for arbitrary layouts. The results are again shown in Figure 8.
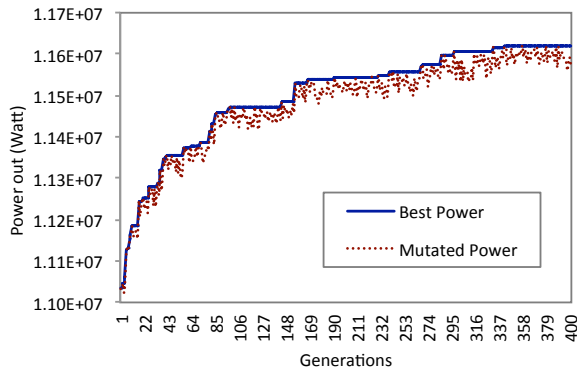
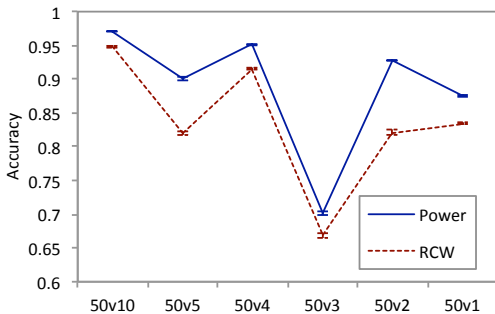**Figure 7: Optimisation results of (1+1)-EA with a simple mutation**

Figure 8: Accuracy of six approximation models for evolving layouts. Shown are the results when 10, 5, 4, 3, 2, and only 1 (of 50) frequencies are used.

The results of both scenarios largely agree. The 10 and 5 frequencies approximations provide the best accuracy and precision in both scenarios. However, we do not choose them due to their relatively higher cost compared with the single frequency approximation. The single frequency (i.e., the prevailing frequency) approximation provides acceptable accuracy and precision with minimal cost, which makes it the ideal trade-off in our case. With incorporating the approximation, the cost of computation is reduced by around 98%, i.e., from around 2,100 minutes to be around 42 minutes for calculating one layout of a 50 WECs array.

3.2   Model Speed-Up Through Caching

Another approach that we introduce along with the single frequency approximation in order to reduce the computational cost is 'caching', which is a technique widely used in software engineering for improving performance. In our particular model, the most frequently used calculations in our MATLAB model are `integral`, `factorial`, and `bessel`. The time spent with such calculations is significant, and a number of them are duplicated during the power computations for a single layout. For instance, in order to calculate the power output of a 50 WECs array, one million calls of `integral` are made, while around 89.5% of them are duplicates. Therefore we cache the results of such calculations into several hash-maps with their parameters hashed to be the corresponding keys. This way, subsequent calls can query the results with their parameters instead of recalculating them. By implementing this technique, the computational cost can be reduced by around 85% without influencing the accuracy.

For calculating one layout of a 50 WECs array mentioned in the previous section, the cost is decreased further from about 42 minutes to about 6 minutes.

4.   COMPUTATIONAL STUDY

In this section we report on our layout investigations of submerged wave energy converters. In the first set of experiments, we considere WECs arranged in a grid-based layout. There, the devices can share mooring points and/or power take-off systems, which results in a significant reduction in capital cost. In the second part, we relax this constraint to investigate layouts where the buoys can be placed arbitrarily, as long as the minimum safety distance is maintained.

4.1   Radii Optimisation

We conduct a range of experiments for optimising the radii of buoys in a staggered array as shown in the introductory Figure 3. In this array, the columns of buoys are spaced 93.33m apart and the rows 107.77m, due to technical reasons. Each buoy in the array can have a different radius of either 2m, 2.5m, 3.2m, 4m or 5m. This quantisation is necessary for both optimisation and also in practice, in order to reduce the number of buoy variants. q-factor is primarily used as the optimisation criterion, although some experiments also consider the relative capture width (Equation 6).

For small array sizes, including 1x1, 1x2, 2x1 and 2x2, it is feasible to use brute force search (BFS) to explore the entire solution space and find the optimal solution. For example, the largest of these small arrays is the 2x2 configuration, which has 625 possible solutions and takes 10 hours to evaluate them all. The best 2x2 configuration has a q-factor of 0.9990 (with a corresponding $\overline{RCW}$ value of 0.6453), which is a layout comprising of two 2m buoys and two 5m buoys. Interestingly, the best-performing 2x2 layout in terms of $\overline{RCW}$ achieved a significantly higher value of 0.7988 (a layout with four 5m buoys), while the q-factor value decreased slightly to 0.9658, see Figure 9. However, this is actually not surprising since the q-factor and $\overline{RCW}$ are two different measures: while $\overline{RCW}$ refers to the maximum power, the q-factor shows to the maximum efficiency of the array in comparison to individual devices. In the model, buoys of different sizes are submerged to the same depth due to constraints of the staggered layout, which affects the efficiency of smaller buoys. Thus, 5m devices submerged to 6 m are more productive in terms of power than 2m buoys submerged to the same depth. As a result, the optimisation using $\overline{RCW}$ ends up with larger WECs. On the other hand, for the q-factor optimisation it is more important to have a constructive hydrodynamic interaction between buoys in the array. Taking into account that in a staggered layout distances between devices are around 100m, values of q-factor are much higher for smaller buoys as at such distances interaction is reduced to a minimum.

The 3x3 array configuration has almost 2 million solutions, meaning that a brute force search is no longer feasible due to the simulation times needed. Yet for smaller arrays sizes, the optimal configuration is found to only consist of buoys with a radius of either 2m or 5m. Using this insight, we are able to conduct a partial BFS of the 3x3 array by examining only those solutions containing 2m and 5m buoys. This partial BFS takes approximately 2 days to complete, but the result is a solution with a q-factor of 0.9956 (see Figure 10), which is comparable to the 2x2 optimal configuration, even though
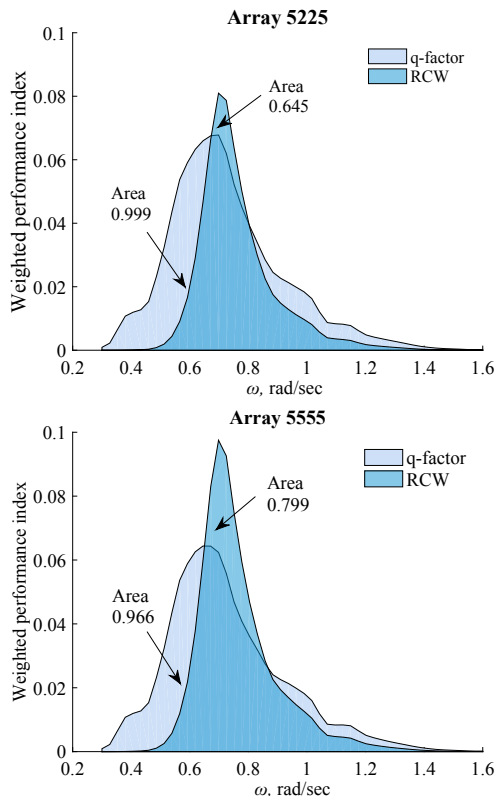
Figure 9: **Comparison of the best performing layouts 5225 and 5555. Shown is the performance for different wave frequencies. The area under the curve corresponds to the expected performance.**
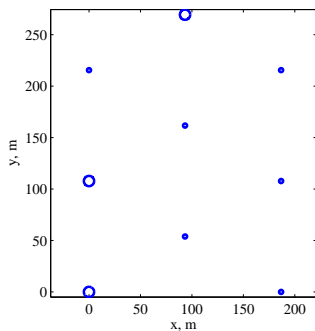

Figure 10: **Best solution found for the 3x3 staggered array. The direction of wave propagation is from left to right. All buoys have diameters of 2m or 5m. q-factor value = 0.9956. $\overline{RCW}$ value = 0.5303. The large 5m buoys make the most of the incoming waves, and the small 2m buoys are most efficient when placed behind the 5m buoys.**

the search was not completely exhaustive in this case.

Since this 3x3 solution found by the partial BFS is not necessarily optimal, we tried using several variants of randomised local search. This did not yield a better 3x3 configuration. An exhaustive evaluation of the local neighbourhood further revealed that this all 2m buoy solution was indeed a local optimum for single changes in the buoy diameters.

We also briefly consider the 4x4 and 5x5 configurations. As BFS has proved to be inefficient, we simply generate all

2m buoy solutions for 4x4 and 5x5, and all of them proved to have q-factors of approximately 0.99. Although these are unlikely to be optimal, the relatively high q-factors show that all 2m buoy solutions may provide configurations with relatively high q-factors for even larger arrays. A similar local neighbourhood check for these 4x4 and 5x5 solutions shows that they are indeed local optima for performing changes to single buoys. This proves that a q-factor is not suitable for the buoy size optimisation at the fixed layout and another performance index should be developed for such a task.

4.2 Placement Optimisation

4.2.1 Experimental Setup

In the following experiments we no longer enforce the grid-like layout from before. We employ two different algorithms to optimise the layouts. The first one is the (1+1)-EA (as used in Section 3), which randomly chooses and moves only one WEC in a layout to a new feasible location. The second algorithm the the Covariance Matrix Adaptation based Evolutionary Strategy (CMA-ES) [14]. CMA-ES self-adapts the covariance matrix of a multivariate normal distribution. This normal distribution is then used to sample from the multidimensional search space where each variate is a search variable. The covariance matrix allows the algorithm to respect the correlations between the variables making it a powerful (and popular) heuristic search algorithm.

Initially, both algorithms place the N buoys randomly in the provided area. In preliminary experiments we found that the regular grid initialisation with maximal distances in the rows and columns to perform similar to the random one. While the grid minimises the interactions by maximising the intra-buoy distance, interestingly the positive interferences appear to outweigh what would intuitively be considered a disadvantage.

Both algorithms take care of the constraints in the following ways. When a layout has buoys which violate the proximity constraint or if a buoy is located outside the allowed area, we resample a new solution in (1+1)-EA and CMA-ES, before invoking the time-consuming simulations. For boundary constraints, CMA-ES rounds the coordinates to the nearest boundary value.

The CMA-ES configuration we use here is as follows. We use a population size of two, which is used to generate two new solutions. We run this (2+2)-CMA-ES for 200 generations, and with an initial standard deviation for each decision variable of 20, based on preliminary experiments. The second algorithm, (1+1)-EA, we run with the same total evaluation budget of 400 evaluations.

4.2.2 Observations

As we now focus on larger arrays, we use the approximate model from Section 3, where only a single frequency is considered. Under the provided conditions, a single isolated 5m buoy has a power output of 5.547e+5 Watts.

Figure 11 shows the results from our optimisation of both the simple (1+1)-EA and the CMA-ES. In both cases, the former produces layouts with significantly higher outputs. Interestingly, this simple algorithm outperforms CMA-ES, even though the later can adapt itself to the problem. It appears that the 200 generations given to CMA-ES are not enough time. To a limited degree this is supported by our observation that CMA-ES begins to converge at the end
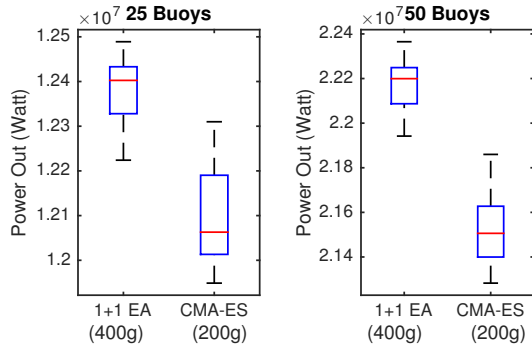
Figure 11: Optimisation results from our 25 and 50 buoys study. Shown are the results of 20 independent runs. For 25 buoys, the initial average q-factor is 0.8123, and the final q-Factors for (1+1)-EA and CMA-ES are 0.8930 and 0.8723. For 50 buoys, the initial average is 0.7267, and the final ones are 0.7995 for (1+1)-EA and 0.7760 for CMA-ES.

of the computation budget provided. By then, the average standard deviation decreases to values of about 4 to 8, which means that large changes to the layouts become increasingly unlikely.

As (1+1)-EA is not able to fine-tune a solution, we take a solution found for 25 buoys and give it to CMA-ES for fine-tuning, with $\sigma = 1.0$ for 200 generations. The resulting layout is shown in Figure 12 and its power output increased by 1.1%. This means that while CMA-ES experiences difficulties in creating good layouts from scratch, it can still be used to tune existing solutions.

In this layout, it is not very surprising that the buoys facing the incoming waves have the highest power output. Further into the farm, the output decreases quickly, because the interactions become increasingly important with increasing number of columns [1]. This is turn shows the fidelity of our optimisation results. The optimisation considers this indirectly, as the density of the buoys on the left hand side of the final layout is significantly higher than the density of buoys in the right hand side. Interestingly, constructive interferences result at times in individual WECs having an above-average output (greater than 5.547e+5 Watts) at certain locations, e.g. the buoy located at $(360, 680)$.

Finally, we briefly demonstrate the applicability of our approach to a very large array. In the single run that we perform (1+1)-EA (again using 400 generations) increases the q-factor significantly by 10.4% over the initial layout. Note that the optimisation with the original model would have taken about 2750 days. The actual optimisation using our speed-ups presented in Section 3 took only 8.3 days, which corresponds to a speed-up by a factor of 330.

We show the final layout in Figure 13. Just as before, the buoys facing the incoming waves have the highest power output. Further into the farm, the output decreases quickly, however, at times positive interferences result in individual turbines having an above-average output.

5. CONCLUSIONS

This study provides first insights into the layout problem of submerged wave energy converters. It is also the first time multiple three tether buoys have ever been investigated.
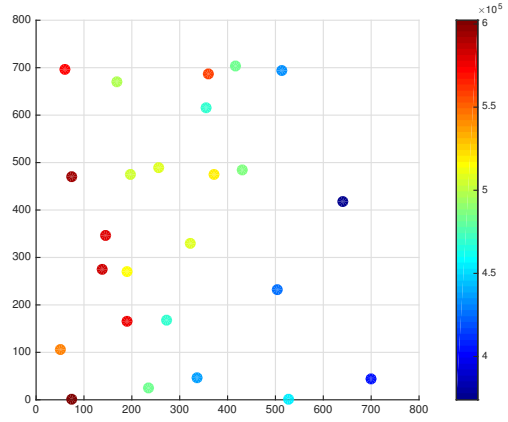

Figure 12: Best layout found for the 25 buoy study. The direction of wave propagation is from left to right. All buoys have diameter 5m, and the area is $0.707 \cdot 0.707 km^2$. The overall power out is 1.257e+7 Watts. The q-factor value is 0.9063 (initially 0.8964) and the $\overline{RCW}$ value is 1.434 (initially 1.252). The colours indicate the power generated by each buoy.
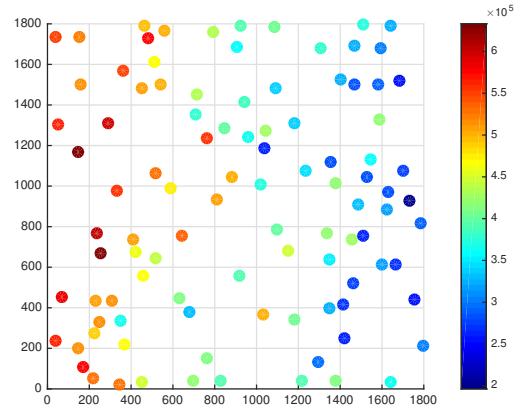

Figure 13: Best layout found for the 100 buoy study. The direction of wave propagation is from left to right. All buoys have diameter 5m, and the area is $1.8 \cdot 1.8 km^2$. The overall power out is 4.147e+7 Watts. The q-factor value is 0.7476 (initially 0.6769) and the $\overline{RCW}$ value is 1.183 (initially 1.071). The colours indicate the power generated by each buoy.

The first simulations of the buoy interactions were computationally prohibitively expensive, taking hours or even days. Through model approximations and caching, we achieved up to 350-fold speed-ups in the simulation times needed. This in turn allowed us to iteratively optimise the interactions in WEC arrays.

Among others, we have made two high-level observations that add to the knowledge of designing such arrays. First, we have discovered a potential design flaw, i.e., buoys of different diameters should not be submerged at the same depth, but the top surface of all buoys should be same distance to the sea surface. Second, we have learned that positive interference can result in higher than normal power outputs for individual buoys. This is surprising, since such effects are hardly ever heard of. For example in wind energy related

research, wake effects and turbulences with their negative effects are well-known, but positive effects are not.

Our next steps include the refinement of the interaction model to allow varying submergence depths. Also, we will revisit the objective function to include economic aspects of the array construction and operation. For example, cost related measures such as the characteristic mass of the buoy and the significant power-take off force relative to the yearly power production can be good indirect cost estimators [2, 3].

In the long-term, we will further speed-up the software side in Matlab, we will consider additional objectives such as stress on the mooring points, which drives capital cost, and we will increase the realism by considering additional incident wave directions. At present, the latter will pose the biggest challenge, as it will come at a significant increase in simulation time.

References

[1] A. Babarit. On the park effect in arrays of oscillating wave energy converters. *Renewable Energy*, 58:68 – 78, 2013.

[2] A. Babarit, J. Hals, M. Muliawan, A. Kurniawan, T. Moan, and J. Krokstad. Numerical estimation of energy delivery from a selection of wave energy converters – final report. Report, Ecole Centrale de Nantes & Norges Teknisk-Naturvitenskapelige Universitet, 2011.

[3] A. Babarit, J. Hals, M. Muliawan, A. Kurniawan, T. Moan, and J. Krokstad. Numerical benchmarking study of a selection of wave energy converters. *Renewable Energy*, 41:44–63, 2012.

[4] S. Bellew, T. Stallard, and P. Stansby. Optimisation of a heterogeneous array of heaving bodies. In *Proceedings of the 8th European Wave and Tidal Energy Conference*, pp. 519–527, 2009.

[5] A. Chertok. Wave-actuated power take-off device for electricity generation. Report, Resolute Marine Energy, 2013.

[6] B. Child and V. Venugopal. Optimal configurations of wave energy device arrays. *Ocean Engineering*, 37: 1402–1417, 2010.

[7] A. de Andrés, R. Guanche, L. Meneses, C. Vidal, and I. Losada. Factors that influence array layout on wave energy farms. *Ocean Engineering*, 82:32–41, 2014.

[8] B. Drew, A. Plummer, and M. N. Sahinkaya. A review of wave energy converter technology. *Proceedings of the Institution of Mechanical Engineers, Part A: Journal of Power and Energy*, 223:887–902, 2009.

[9] A. F. O. Falcão. Wave energy utilization: A review of the technologies. *Renewable and Sustainable Energy Reviews*, 14:899–918, 2010.

[10] J. Falnes. *Ocean waves and oscillating systems: Linear interactions including wave-energy extraction.* Cambridge University Press, 2002.

[11] C. Fitzgerald and G. Thomas. A preliminary study on the optimal formation of an array of wave power devices. In *Proceedings of the 7th European Wave and Tidal Energy Conference*, 2007.

[12] P. B. Garcia-Rosa, G. Bacelli, and J. V. Ringwood. Control-informed optimal array layout for wave farms. *IEEE Transactions on Sustainable Energy*, 6:575–582, 2015.

[13] J. Hals, J. Falnes, and T. Moan. A comparison of selected strategies for adaptive control of wave energy converters. *Journal of Offshore Mechanics and Arctic Engineering*, 133:031101, 2011.

[14] N. Hansen and A. Ostermeier. Adapting arbitrary normal mutation distributions in evolution strategies: the covariance matrix adaptation. In *Proceedings of IEEE International Conference on Evolutionary Computation*, pp. 312–317, 1996.

[15] M. A. Hemer and D. A. Griffin. The wave energy resource along Australia's southern margin. *Renewable and Sustainable Energy*, 2, Art. 043108, 2010.

[16] M. Lagoun, A. Benalia, and M. Benbouzid. Ocean wave converters: State of the art and current status. In *IEEE International Energy Conference*, pp. 636–641, 2010.

[17] C.-H. Lee. *WAMIT Theory Manual.* Massachusetts Institute of Technology, 1995.

[18] C. Linton. Radiation and diffraction of water waves by a submerged sphere in finite depth. *Ocean Engineering*, 18:61 – 74, 1991.

[19] I. López, J. Andreu, S. Ceballos, I. M. de Alegría, and I. Kortabarria. Review of wave energy technologies and the necessary power-equipment. *Renewable and Sustainable Energy Reviews*, 27:413–434, 2013.

[20] P. A. Lynn. *Electricity from Wave and Tide: An Introduction to Marine Energy.* John Wiley & Sons, 2013.

[21] L. Mann, A. Burns, and M. Ottaviano. CETO, a carbon free wave power energy provider of the future. In *Proceedings of the 7th European Wave and Tidal Energy Conference*, 2007.

[22] L. D. Mann. Application of ocean observations & analysis: The CETO wave energy project. In *Operational Oceanography in the 21st Century*, pp. 721–729. Springer, 2011.

[23] A. McCabe, G. Aggidis, and M. Widden. Optimizing the shape of a surge-and-pitch wave energy collector using a genetic algorithm. *Renewable Energy*, 35: 2767–2775, 2010.

[24] M. Mohamed, G. Janiga, E. Pap, and D. Thévenin. Multi-objective optimization of the airfoil shape of Wells turbine used for wave energy conversion. *Energy*, 36:438–446, 2011.

[25] G. Nunes, D. Valério, P. Beirao, and J. S. Da Costa. Modelling and control of a wave energy converter. *Renewable Energy*, 36:1913–1921, 2011.

[26] S. H. Salter. Wave power. *Nature*, 249:720–724, 1974.

[27] J. T. Scruggs, S. M. Lattanzio, A. A. Taflanidis, and I. L. Cassidy. Optimal causal control of a wave energy converter in a random sea. *Applied Ocean Research*, 42:1–15, 2013.

[28] N. Y. Sergiienko, B. S. Cazzolato, B. Ding, and M. Arjomandi. Frequency domain model of the three-tether WECs array. https://www.researchgate.net/publication/291972368_Frequency_domain_model_of_the_three-tether_WECs_array, 2016. [Online; accessed 2-February-2016].

[29] M. A. Srokosz. The submerged sphere as an absorber of wave power. *Fluid Mechanics*, 95:717–741, 1979.

[30] G. X. Wu. Radiation and diffraction by a submerged sphere advancing in water waves of finite depth. *Proceedings: Mathematical and Physical Sciences*, 448: 29–54, 1995.